BULLETIN OF THE POLISH ACADEMY OF SCIENCES
TECHNICAL SCIENCES
DOI: 10.24425/bpasts.2024.151678

A random field-based simulational identification of possible levels of material imperfections of adhesive-bonded joints

Karol Winkelmann[1]*, Faizullah Jan[1], Łukasz Smakosz[1], Violetta Konopińska-Zmysłowska[1], Victor Eremeyev[2], Marcin Kujawa[1]

[1] Gdansk University of Technology, Faculty of Civil and Environmental Engineering, Poland
[2] University of Cagliari, Faculty of Civil Engineering and Architecture, Italy

Abstract. Recently, structural adhesives have become significant in the shaping of structural elements, especially in thin-walled structures, where they replace or supplement traditional connection methods. However, adhesive-bonded joints are highly susceptible to internal structural imperfections due to their application technique and the nature of the adhesive. These material inconsistencies impact the strength parameters and the mechanical behavior of the entire connection. This study proposes a simplified method for the probabilistic numerical modeling of structural imperfections in an adhesive layer. The adhesive is modeled as an uncorrelated random field with weakened elements representing structural imperfections randomly scattered throughout its entire volume. The percentage of these imperfections (in relation to the total volume) is adopted a random variable. By conducting experimental tests on dogbone specimens of a selected adhesive and comparing them to adequate numerical tests with varying volumes of weakened elements, the determination of the representative imperfection volume of the investigated adhesive was possible. Based on these tests, the calibration of the probability density function to describe the volume of the imperfections may be performed. Furthermore, the application of the random model for an adhesive-bonded single lap-joint is shown to be viable. Finally, the calculation of a probability-based mechanical response (in this case, the normal force at critical elongation) of the single lap-joint with structural imperfections is performed, and its resultant reliability is assessed and evaluated.

Key words: adhesive-bonded joints, adhesive imperfections, random fields, probabilistic analysis, reliability

SYMBOLS AND ABBREVIATIONS

$\beta(p)$ – reliability index of the single lap joint, given a random level of adhesive imperfections p
δ_{3f} – effective plastic displacement at failure of the adhesive
ε_{3f} – strain at plastic fracture of the adhesive
ε_{3u} – strain at rupture of the adhesive
ε_{lim} – relative limit strain of the single lap joint
λ – scale factor of a two-parameter Weibull distribution
μ_i – mean value of a given result; i=F_{exp}, $F_{num,p}$, p
ν_i – Poisson's ratio: i=1, 2 for adherends, i=3 for adhesive
σ_i – standard deviation of a given result; i=F_{exp}, $F_{num,p}$, p
σ_{triax} – stress triaxiality parameter
b – width of a single lap joint
exp – denominator of the experimental test results
f_{iu} – ultimate strength under axial tension: i=1, 2 for adherends, i=3 for adhesive
f_{iy} – yield strength: i=1, 2 for adherends, i=3 for adhesive
$f_X(x)|_{Wb}$ – two-parameter Weibull distribution PDF
k – shape factor of a two-parameter Weibull distribution
l – length of a single lap joint
m_i – mode of a given result; i=F_{exp}, $F_{num,p}$, p
num – denominator of the numerical test results
p – random variable representing the level (percentage) of adhesive imperfections
p_{min}, p_{max} – lower and upper bounds of the generated levels of imperfections
r – correlation coefficient
s_i – scatter of a given result; i=F_{exp}, $F_{num,p}$, p
t_i – thickness of a given layer in the single lap joint: i=1, 2 for adherends, i=3 for adhesive
u=u_x – horizontal displacement of the single lap joint
u_h=u_{hx} – relative horizontal displacement of the single lap joint
v_i – coefficient of variation of a given result; i=F_{exp}, $F_{num,p}$, p
x_i – random field data points
A_{joint} – cross-sectional area of the adhesive layer in the joint
E_i – Young's modulus: i=1, 2 for adherends, i=3 for adhesive
F – rupture force (for the adhesive specimen) or ultimate tensile force (for the adhesive-bonded single lap joint)
F_{exp} – experimental test result of the rupture tensile force
F_{id} – rupture tensile force for the adhesive free of imperfections
$F_{num,min}$, $F_{num,max}$ – lower and upper bounds of the numerical test results of the rupture tensile force

*e-mail: karolwin@pg.edu.pl (Corresponding Author)

$F_{num,p}$ – numerical test result of the rupture tensile force of an adhesive specimen with an imperfection level of p
$F(p)$ – linear approximation function of the relationship between the imperfection level p and the axial tensile force F
FORM – First Order Reliability Method
LSF – limit state function
N_{perm} – permissible value of the tensile force in the joint with adhesive imperfections
PDF – probability density function
R^2 – determination coefficient
$U(0,1)$ – standard uniform distribution
V_i – variance of a given result; i=F_{exp}, $F_{num,p}$, p
V_{imp} – total volume of structural imperfections present within the entire adhesive domain
V_{tot} – total volume of the adhesive
$X(x_i)$ – uncorrelated one-dimensional random field

1. INTRODUCTION

The concept of using adhesively bonded connections instead of traditional methods like screws or welding, and forming thin-walled metal structural members (such as beams and columns) by joining two or more cold-rolled steel channels with structural adhesives, remains an innovative idea, particularly in civil engineering [1].
Adhesive-bonded joints of thin-walled members may, in some cases, be advantageous over traditional connections in various technological areas. For example, the connection region does not need to be weakened by screw holes or residual welding stresses, the method of making the connections is relatively easy, and the overall geometry of the joint is simpler. However, primarily due to the nature of the adhesive and the challenges related to proper manufacturing and application of the adhesive to the adherends, the internal structure of the adhesive may become non-uniform and heterogeneous, to a certain, unneglectable extent. Microscopic views displaying overall internal structural imperfections of an adhesive material and layer are shown in Fig. 1.
As indicated in Fig. 1, several structural imperfections (heterogeneities), such as pores (bubbles of air) are clearly visible. In some cases, there might be also foreign inclusions, particle pollution, delamination, phase separations, and other imperfections. These heterogeneities are unintentionally formed in the adhesive layer during mixing, setting, thermal cycling, shrinkage processes, curing, etc., or are directly induced by human errors [2].
The occurrence of the abovementioned imperfections introduces severe uncertainties regarding material strength properties and parameters, which subsequently produce significant variability in all types of possible structural mechanical responses of adhesive-bonded connections. Examples of such response include load-bearing capacity, long-term durability, susceptibility to fatigue, behavior in low and high temperatures, creep initiation time, critical elongation and overall performance (e.g. in terms of serviceability) of the adhesive-bonded joint [3, 4, 5]. Moreover, the contribution of a given type of uncertainty to the final joint response variability should be considered individually in a specific test environment (an in-depth uncertainty quantification is strongly advised), as the overall variability depends on a number of individual factors closely related to a given execution processes of the adhesive layer [6]. All these aforementioned remarks are the main obstacles severely impeding the utilization of members with adhesive-bonded joints and preventing the technology from becoming widespread [7].

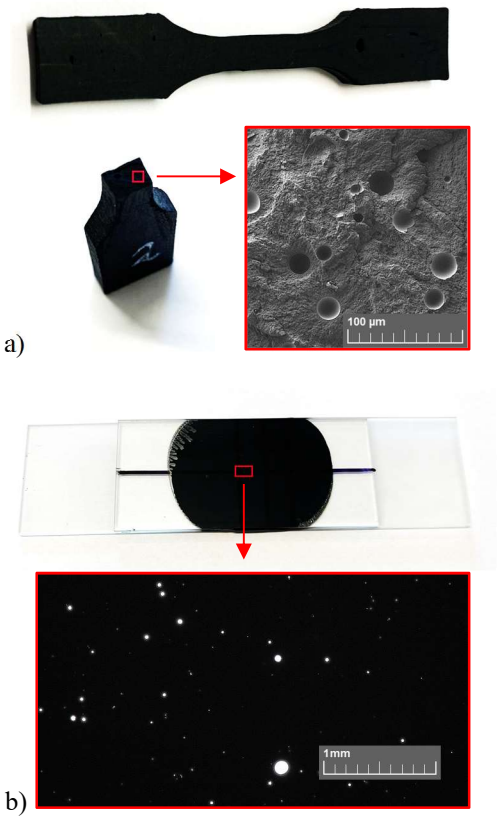

Fig.1. Microscopic views of internal structural imperfections in: (a) the fracture surface of an adhesive-cast dogbone specimen, (b) a thin adhesive layer spread between two adherends.

Thus, before employing adhesive-bonded joints in real thin-walled members on an industrial scale, it is necessary to perform advanced theoretical and numerical research regarding the overall performance of such connections, preferably of a probabilistic nature. As finite element analysis (FEA) plays a fundamental role in their design, particularly detailed numerical modeling of the adhesive layers is of key importance, and it should account for the randomness of the entire layer in detail. The resultant random FE model of the layer must allow the prediction of its performance, specifically in the identification of the limit states (such as exceeding permissible stresses, cracking, and debonding) of thin-walled structural elements assembled with adhesive-based bonds [2, 3, 6].
Many approaches to FE modelling of the material accounting for the randomness in its internal structure are currently developed in the literature, including real-life scale [8], meso-scale [9] or micro-scale [10] approaches and applications. However, they all require extensive experimental tests or sophisticated FE models, which makes the analysis complex and time-consuming.

In another approach, numerous studies in the literature suggest adjusting the material parameters for imperfect or weakened adhesives by filling the material volume with randomly scattered "zero-elements", representing pores and other cavities in the material [6]. It is stated that "zero-elements" should either be absent from the FEM mesh, or their respective material parameters should be visibly lower than nominal to ensure that the mechanical behavior of the imperfect material significantly deviates from its original state.

In line with these remarks, a relatively simple random FE model based on spatially uncorrelated heterogeneous random field approach is proposed in the paper, derived from the observations on the possibility of adequate random modelling of a non-homogeneous material [11]. To fit the precise case of adhesive bonding, the proposed approach of random FE numerical modeling of the adhesive-bonded layer is validated and calibrated on straightforward experimental tests performed on the structural epoxy adhesive 3M Scotch DP490.

2. RANDOM FE MODELLING OF THE IMPERFECT ADHESIVE MATERIAL

As discussed in the introduction, the scatter of the data acquired from real-life experimental tests on adhesive material specimens or adhesive-bonded joints can be directly attributed to the dominant influence that structural imperfections exert on the variation in the mechanical response of the adhesive. Therefore, using an idealized material in finite element modeling of adhesives for real engineering structures is not appropriate. Instead, an FE model that accounts for the imperfect material structure is recommended.

The paper proposes an alternative, straightforward random FE model that is easy to apply to any type of FEM analysis. By coupling the random model with experimental results, the proposed model is expected to reproduce a real-life randomness of a given adhesive. Moreover, the incorporation of the random methodology into the FE model is relatively easy and does not make the processing of the model overly time-consuming or computationally intensive.

The algorithm can be divided into eight distinct steps. Their sequence is proposed below; however, the arrangement of the steps may be subject to change depending on the chosen approach for a given analysis case.

The first step of the proposed algorithm involves the compilation of the FE model. The model of the adhesive specimen is created in the chosen FEA software, determining the total number of FE elements representing the adhesive. This number should be closely coupled with the dimensions of the adhesive volume, employing an element size comparable to the dimension of a possible structural imperfection.

In the second step, a random field is generated. At this stage, an uncorrelated non-homogeneous one-dimensional random field is created, with the number of data points equal to the number of finite elements representing the adhesive in the model. For every data point of the field x_i, a random, non-correlated value is generated from the standard uniform distribution $X(x_i) \sim U(0,1)$ and assigned to this data point. A sample random field generated accordingly, with 101 data points, is shown in Fig. 2.

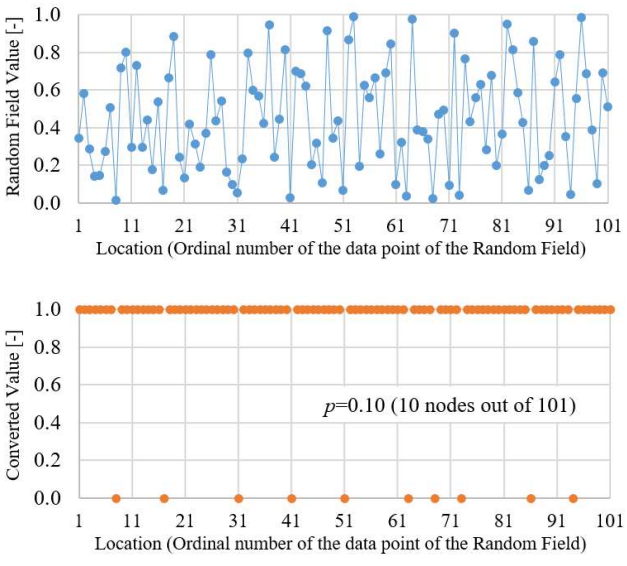

Fig.2. An exemplary 101-data point non-homogeneous uncorrelated one-dimensional random field: (a) output generation, (b) conversion to zero-unit two-point scalar field.

In the third step, the imperfection level denominator, p, is assumed. The value of $p \in (0,1)$ governs the relationship between the total volume of structural imperfections present within the entire adhesive domain (V_{imp}) and the total volume of the adhesive (V_{tot}). It is defined such that $p = V_{imp}/V_{tot}$. The p parameter is represented by a random variable described with a two-parameter non-symmetrical Weibull distribution, often used in similar investigations on imperfect materials [11], with a probability density function (PDF) $f_X(x)|_{Wb}$ given by Eq. (1):

$$p = f_X(x)|_{Wb} = \\ = (k/\lambda)\, e^{-(x/\lambda)^k} (x/\lambda)^{(k-1)} \quad (\text{for } x > 0) \quad (1)$$

where k denotes the shape and λ – the scale factors of the PDF.

In the fourth step one converts the generated random field into a two-point scalar field based on the p value. This means that the $(1-p)\times 100\%$ of random field data points with the highest numerical values are elevated to a unit (1), while the remaining $p\times 100\%$ of data points have their values reduced to zero (0). This conversion is shown in Fig. 2b.

The fifth step is to compile two different FE material models. First, compile a model, later designated as "nominal," which represents the default material used in the model of the "ideal" specimen. This model denotes an isotropic material with no imperfections. Then, compile the second material, later designated as "imperfect", to reflect possible structural imperfections. It should be noted, that if the FEA software allows, a "zero material" can be used for the "imperfect" material, causing the finite elements governed by this model to disappear. Otherwise, a "weakened" material may be used, with relevant parameters derived directly from the "nominal" material through simple mathematical scaling. The finite elements labeled with random field nodal values of 1 are described by the "nominal" material, while the remaining elements labeled with zero are described as the "imperfect" or "weakened" material.

In the sixth step, in order to calibrate the key parameters of the Weibull distribution in Eq. (1), a selected number of trial tests on imperfect FE models, referred to as "confidence intervals" is conducted. In these tests, the p values may be adopted *a priori*, independent of the Weibull PDF, as long as they accurately reflect the behavior of the FE model of the adhesive specimen at specific levels of structural imperfections. For each adopted trial p value, a sufficiently large number of different FE model simulations should be performed to accurately determine the statistical parameters of the model response within the given interval. The changes in the statistical parameters in between given imperfection levels may be approximated (e.g. linearly).

In the seventh step, one conducts real-life calibration tests on given specimens. If needed (e.g. for the determination or verification of basic material and strength parameters), the experimental phase may be conducted at the start of the analysis. Using the experimental results, their statistical parameters are directly compared with the statistical parameters of the FE model trial calculations. Based on the comparison, the key parameters of the Weibull distribution are estimated. This ensures that the p value, when ultimately randomly generated from the distribution, independent of the "confidence intervals", will accurately reflect the real-life variability of the investigated structural response (e.g. stress levels or total elongation at given tensile force value, rupture force, total elongation at failure) exhibited by the experimentally tested adhesive.

In the final, eight step, one transfers the p random variable to FE analysis of real-life joints or elements. As a result, the generated FEM model, based on a simply defined adhesive layer, precisely reflects the adhesive, including specified random imperfections unique to the adhesive used. Thus, the randomized FE model is bound to produce trustworthy structural response parameters with possible and reasonable scatter.

The proposed algorithm has been applied to 3M Scotch DP490 epoxy adhesive. The key results and observations from preliminary tests on dogbone specimens were used to assess the operational reliability of an adhesive-bonded single lap-joint.

3. THE COMPILATION AND THE EXPERIMENTAL CALIBRATION OF THE RANDOM FE MODEL OF A DOGBONE SPECIMEN CAST FROM THE 3M SCOTCH DP490 ADHESIVE

3.1. Description of the dogbone specimen used in the analysis.

As mentioned earlier, the 3M Scotch DP490 adhesive was chosen for the analysis. The selected adhesive was taken into consideration in the form of cast dogbone specimens. The dimensions of a single dogbone specimen are shown in Fig. 3a. First, the specimens were fabricated using the given epoxy adhesive for experimental tests (as shown in Fig. 3b), in order to assess relevant strength and material parameters in a series of tests described in Subsection 3.2.

Furthermore, the investigated dogbone samples were numerically modelled in the ABAQUS FEA commercial software (the visualization of the FE model is presented in Fig. 3c), with the details of the FE modelling collected and adequately explained in Subsection 3.3.

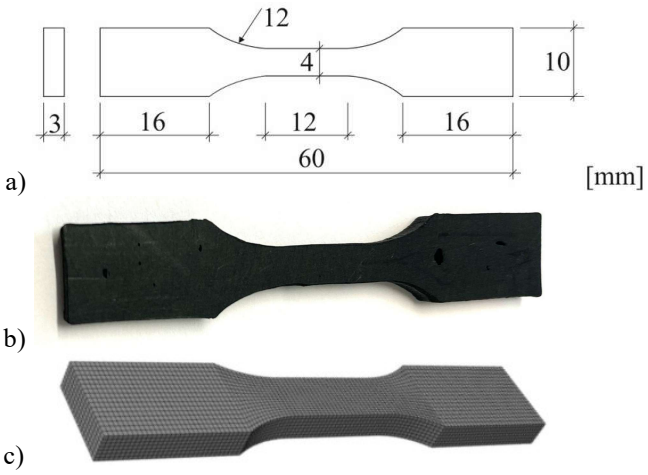

Fig.3. The analyzed dogbone specimen cast from the 3M Scotch DP490 adhesive: (a) specimen dimensions, (b) photograph of a real-life specimen (c) visualization of the numerical FE model of the specimen compiled in ABAQUS FEA commercial software.

3.2. Experimental verification of the "nominal" material parameters of the adhesive.

A decision was made by the Authors to begin the analysis with a series of experimental studies conducted over a population of 25 dogbone specimens meeting the description in Fig. 3a in order to verify the values of key material and strength parameters of the 3M Scotch DP490 epoxy adhesive.

Uniaxial tensile tests were conducted at a constant displacement rate of 0.1 mm/min. The tensile force was measured by a load cell, and sample elongation by an optical extensometer. Engineering strain was calculated as the ratio of elongation to the initial gauge length, and engineering stress as the ratio of applied force to the initial cross-sectional area.

In result, selected stress-strain curves for the experimentally analyzed real-life specimens subjected to uniaxial tension test until rupture are given in Fig 4. Young's modulus was calculated from the initial linear portion of each curve, up to 0.01 strain. Moreover, a numerically-fitted experimental test average is shown in Fig. 4 along with a lower envelope of the experimental stress-strain curves, as this envelope was used to determine the experimental material parameters, subsequently labeled as "nominal".

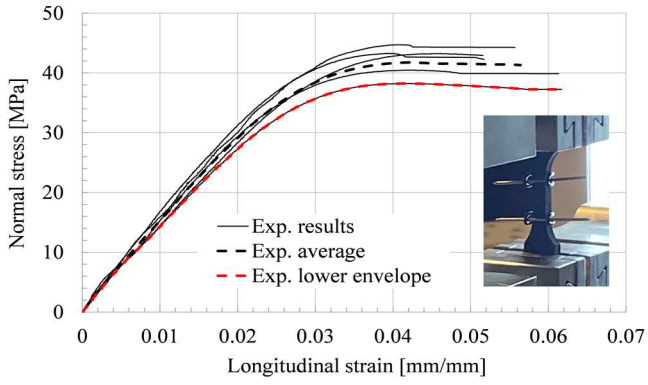

Fig.4. Selected stress-strain curves for the experimentally analyzed real-life samples, a numerically-fitted experimental test average and lower envelope.

Based on the lower envelope of the experimental tests the following values were assessed as "nominal": Young's modulus E_3=1,560 MPa; ultimate strength under axial tension, f_{3u}=38 MPa; yield strength, f_{3y}=28.5 MPa; and strain at rupture, ε_{3u}=0.04. The Poisson's ratio ν_3=0.38 was obtained from the literature [12]. The detailed statistical analysis of the experimental test results is provided in Table 1.

TABLE 1. Experimental test results

	Rupture force [N]	Rupture stress [MPa]	Young's modulus [MPa]
Minimal	620.3	38.2	1,559
Maximal	696.4	44.7	1,647
Mean	662.8	42.0	1,613
Median	667.7	43.2	1,620
Scatter	76.1	6.5	88.0
St. dev.	31.9	2.6	33.4

3.3. Compilation of the numerical FE model of the dogbone test specimen.

In the subsequent step of the analysis, for the purpose of the introduction of the random FE model of the adhesive, a computational numerical model of the "ideal" specimen was first compiled in the ABAQUS FEA commercial software.

The 3D dogbone specimen FE model was defined with a total of 13,216 C3D8R finite elements (three-dimensional, 8-node hexahedral elements with reduced integration and hourglass control). The approximate element size was 0.5 mm.

A "nominal" material model was assumed throughout the entire specimen, with the adoption of the experimentally derived parameters. The "nominal" stress-strain curve was obtained using the Ramberg-Osgood law for the data from the lower envelope of experimental tests. The material model was defined in ABAQUS FEA software as linear elastic until reaching yield strength, f_{3y}. The plastic range was defined with von Mises yield criterion. Ductile failure initiation was defined with a stress triaxiality of σ_{triax}=–0.333 MPa, and a strain at plastic fracture of ε_{3f}=0.05. Linear damage evolution was used, with effective plastic displacement at failure equal to δ_{3f}=1 mm.

It is worth noting that the established material parameters remain constant within each individual element domain, resulting in a model with 13,216 distinct sets of material parameters. In subsequent calculations, this assumption allows a single data point of an uncorrelated random field to govern the properties of only one element at a time, facilitating a random description of the material throughout its entire volume.

Fixed boundary conditions were applied to both ends of the model, except for translation along the specimen's length at the end where the load was applied (see Fig. 5a). The load was applied by displacing one end of the sample by 2 mm (as also shown in Fig. 5a). A maximum step increment of 0.01 was used to minimize convergence problems. As a result, a force of F_{id}=690 N was obtained as the total reaction force at the support, reaching its maximum value before the failure initiation criterion was met, resulting in a gradual decrease in reaction force. This force value was interpreted as the time step at which the dogbone specimen would break.

The key results from the numerical FE model calculations for the final time steps of the analysis are shown in Figs. 5b-e, both before failure (displacements, maximal logarithmic strain, von Mises stresses, see Figs. 5b-d) and after failure (ductile damage initiation, see Fig. 5e).

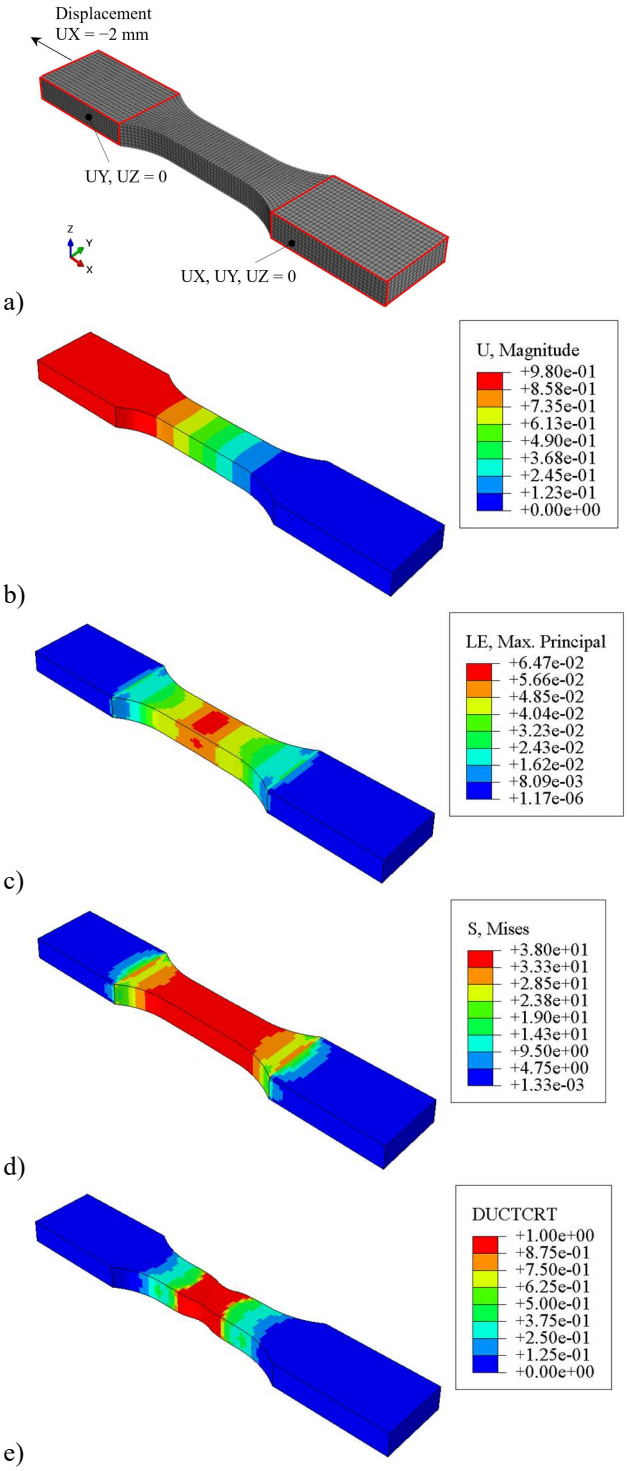

Fig.5. The FE model of the ideal dogbone specimen: (a) geometry, boundary conditions and load, and the results from the time-steps before failure: (b) displacement magnitude [mm], (c) maximal principal logarithmic strain [-], (d) von Mises stress [MPa], and after failure: (e) ductile damage initiation (1 – criterion met).

3.4. Adoption of a "weakened" material to account for the possible structural imperfections.

In the following analysis, it is assumed that the "weakened" elements exist, and their respective material parameters values are directly derived from the "nominal" values described in Subsection 3.2. A simple yet permissible *a priori* assumption was made that the "weakened" values of Young's modulus and ultimate strengths are 10% of their "nominal" counterparts. This relationship is illustrated in Fig. 6, which shows the stress-strain curves for both the "nominal" and "weakened" materials.

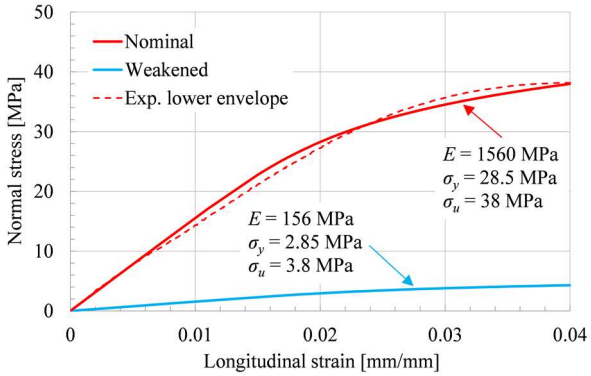

Fig.6. Material stress-strain curves for both the "nominal" and "weakened" materials used in the FE model compared with lower envelope of experimental results.

3.5. Determination of "confidence intervals" – analysis of FE models of dogbone specimens with given volumes (levels) of imperfections.

With the "nominal" and "weakened" materials properly described and implemented in the FEA software, the randomization of the model can be initiated. As discussed in Section 2, the compilation of a FE random model devoted to the tested adhesive for future real-life applications should start with the comparison and calibration of the statistical parameters of the FE model trial calculations with the statistical parameters of the experiments presented in Subsection 3.2.

For this preliminary analysis, 25 non-homogeneous uncorrelated random fields bound by the uniform distribution $X(x_i) \sim U(0,1)$ were generated. Each field consisted of 13,216 data points to match the number of FE elements representing the adhesive in the FE model, as noted in Section 2.

It was decided, that five discrete scenarios involving the presence of imperfections would be analyzed. The p values for each scenario were assumed to be 0.05, 0.10, 0.15, 0.20, and 0.25, respectively, resulting in the generation of dogbone specimen FE models with 5%, 10%, 15%, 20%, and 25% of their respective volumes comprised of randomly distributed "weakened" elements, with their material and strength parameters replaced by the values discussed in Subsection 3.4. For each imperfection volume scenario, an equal number of five distinct FE models (labeled as "samples" in probabilistic methodology) were generated and analyzed (based on five different random fields, converted to zero-unit discrete fields for the purpose of the task, as previously noted), thus constituting the aforementioned number of 25 random fields generated and converted in total. This task was carried out using a proprietary algorithm developed in MATLAB commercial software.

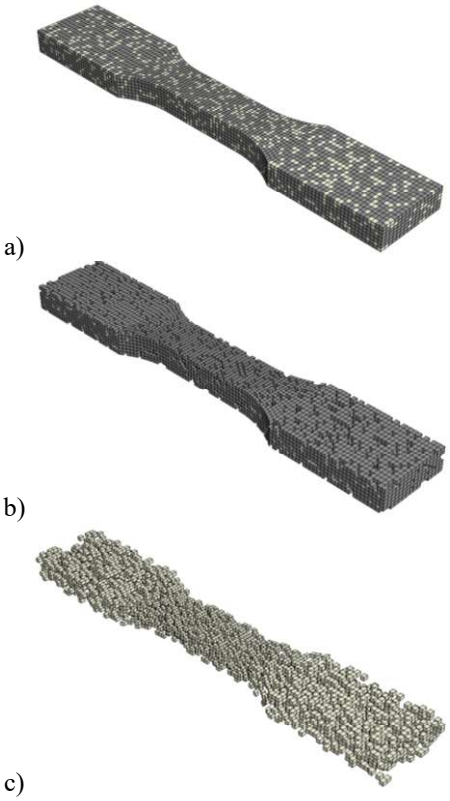

Fig.7. An exemplary FE model of the imperfect dogbone specimen, assuming 25% of the entire sample volume was randomly "weakened" (as indicated by a brighter color): (a) the entirety of the sample, (b) elements with "nominal" parameters, (c) elements with "weakened" parameters.

For clarity, Fig. 7 presents a representative numerical sample from the set generated for the variant with 25% structural imperfections. Figs. 7b-c also illustrates the breakdown of the entire sample into "nominal" and "weakened" elements.

Next, full FEA was conducted for each sample generated in every variant with structural imperfections in the FE model. Calculations were performed, as already mentioned, for each of the 5 calculation variants (each arbitrarily chosen imperfection volume level) consisting of 5 randomly generated distributions of "weakened" elements, resulting in a determined set of 25 force-elongation curves for the analyzed samples corresponding to the represented variants. The curves are shown in Fig. 8.

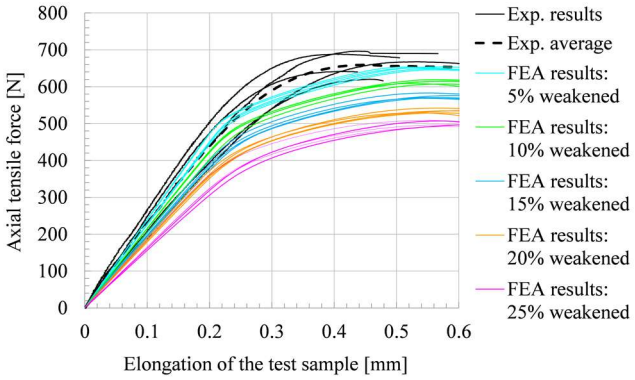

Fig.8. Selected force-elongation curves for the analyzed specimens corresponding to the represented variant incorporating different levels of structural imperfections.

Moreover, the rupture force value was obtained using the FEA software for each random sample, in the same manner as shown in Subsection 3.3. To better visualize the comparison between the performance of the "ideal" and the "imperfect" specimen, key results similar to those given in Fig. 5 for a perfect specimen are presented in Fig. 9 for the FE model calculation of an "imperfect" specimen (with 5% "weakened" elements).

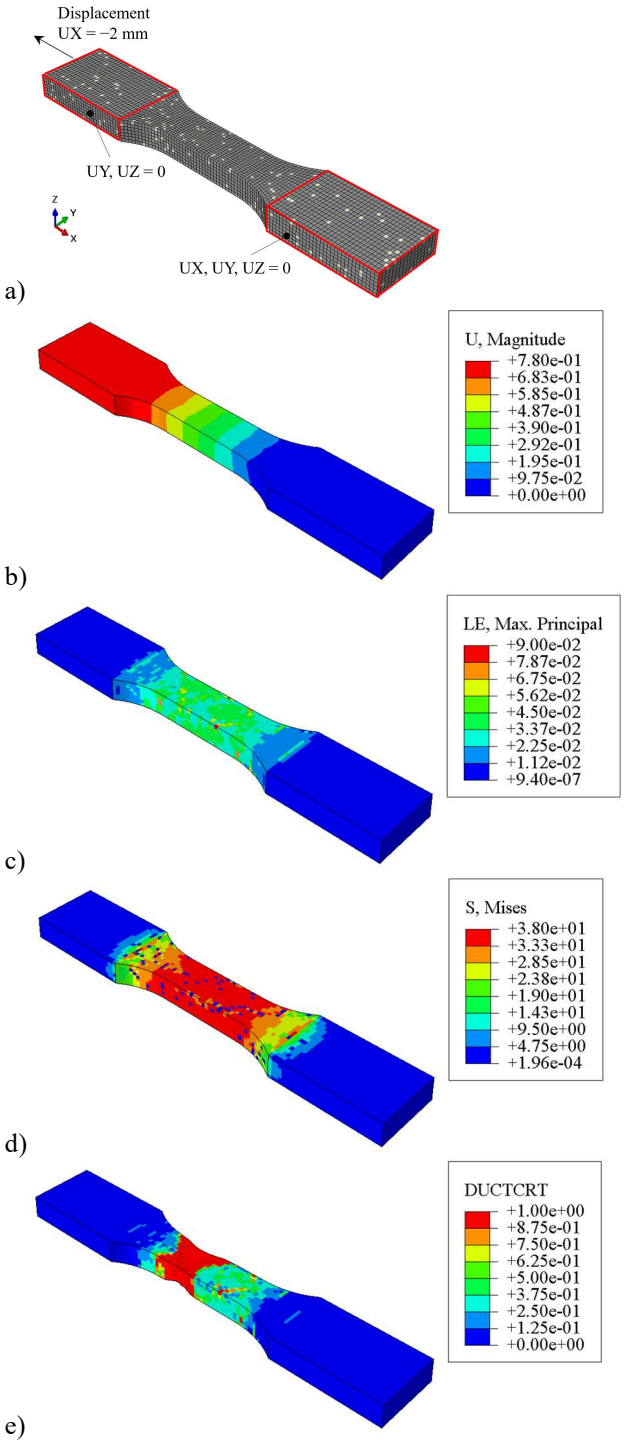

Fig.9. Results of DBS numerical model with 5% of "weakened" elements (example): (a) geometry, boundary conditions and load, and the results from the time-steps before failure: (b) displacement magnitude [mm], (c) maximal principal logarithmic strain [-], (d) von Mises stress [MPa], and after failure: (e) ductile damage initiation (1 – criterion met).

It is worth noting, that the rupture force was chosen as the primary structural response of the dogbone specimen due to its consistency with the nature of the load. In random terms, the rupture force represents the output response random variable. For each "confidence interval", five different rupture force values are determined, allowing for the calculation of statistical parameters. Consequently, the mean value and standard deviation of the random response were computed for each variant. These results are presented in Table 2.

TABLE 2. Probabilistic parameters of the response of FE models of the dogbone test specimens with structural imperfections

Volume (level) of structural imperfections in the FE model	Rupture force F [N]			
	Maximal	Minimal	Mean value	Standard deviation
5% (p=0.05)	653.8	645.6	650.4	3.1
10% (p=0.10)	619.2	607.2	613.1	4.5
15% (p=0.15)	582.8	568.5	573.7	5.2
20% (p=0.20)	542.2	528.9	534.2	4.8
25% (p=0.25)	509.0	492.0	500.5	6.4

Based on the data presented in Table 2, a noticeable decrease in mean rupture force is observed with an increase in the total volume of imperfect elements in the entire FE model domain. Simultaneously, there is a slight increase in standard deviation. Therefore, is it concluded that the mean values of ultimate tensile forces from the FE analysis can serve as the basis for assessing the volume of material structural imperfections in real-life elements, while the standard deviation can help anticipate result variability.

3.6. Adjustment of statistical parameters from experimental tests and FEA-derived "confidence intervals" to determine the key parameters of the Weibull distribution of structural imperfection volumes (levels).

As expected, the FEA-based "confidence intervals" allow for the comparison of the mean rupture force value from experimentally tested specimens and numerical calculations, which is essential for subsequent real-life applications.

The mean value of experimentally derived rupture forces was determined to be μ_{Fexp}=662.8 N. In parallel, FEM computations determined the rupture force to be F_{id}=690 N for a model without any imperfections (p=0), as discussed in Subsection 3.3. For a set of models with 5% imperfect elements in the entire FEM volume (p=0.05), the mean rupture force was $\mu_{Fnum,0.05}$=650.4 N, as shown in Table 2. A linear interpolation on the results was then performed, resulting in a rupture force value of $F_{num,0.035}$=662.3 N. This value corresponds to a presumed, non-calculated scenario where the entire FEM volume comprises approximately 3.5% imperfect elements. Consequently, using the "confidence intervals", the average rupture force determined in the experimental test is numerically approximated by a set of random samples with an average imperfection level of p=0.035.

However, it should be noted that both the scatter (s_{Fexp}=76.1 N) and the standard deviation (σ_{Fexp}=31.9 N) of the experimentally assessed rupture forces are very high (see Table 1). This indicates that with an increase in the number of specimens, a relatively low rupture force may be observed, potentially even lower than the lower envelope shown in Fig. 4. To account for the possibility of such a "faulty" specimen, the 3-sigma rule was applied, resulting in a marginal rupture force calculated as F_{id}–3σ_{Fexp}=577.2 N. In the performed "confidence intervals" assessment, this expected rupture force value falls between the scenarios for 10% "weakened" elements in the entire adhesive volume ($\mu_{Fnum,0.10}$=613.1 N) and 15% "weakened" elements ($\mu_{Fnum,0.15}$=573.7 N). A linear interpolation between these bounds results in a rupture force value of $F_{num,0.145}$=577.6 N, corresponding to a presumed, non-calculated scenario where imperfections constitute up to 14.5% of the entire adhesive volume in some numerical samples. This value, although significantly lower than the experimental minimum value of 620.3 N (see Table 1), is recommended for engineering-safe design considerations.

By determining the mean value of structural imperfection volume (p=0.035, representing 3.5% of "weakened" elements in the entire FE domain) and the maximum possible imperfection volume (p=0.145, representing 14.5% of "weakened" elements in the entire FE domain), it is assumed that the natural variability of the adhesive can be predicted based on the comparison of experimental tests with numerical confidence intervals. The key probabilistic parameters of the Weibull probability density function (PDF) given in Eq. (1) can be proposed to transform the *a priori* p values from the intervals into a continuous random variable governing the natural possible volume of the imperfect ("weakened") material. A Weibull PDF with a mean value close to 0.035 is desired, and the distribution should allow for the generation of a value of 0.145 with a marginal (close to zero) probability. A Weibull PDF with a shape factor k=2 and scale factor λ=0.04 meets both criteria. It is described by Eq. (2) :

$$p = f_X(x) = 1250\, e^{-625\,x^2}\, x \quad (\text{for } x > 0) \quad (2)$$

The calibrated distribution yields the following probabilistic moments for the random variable p: mean value μ_p=0.0354491; mode m_p=0.0282843; standard deviation σ_p=0.0185301; and variance V_p=0.000343363. The Weibull PDF described by these values is shown in Fig. 10.

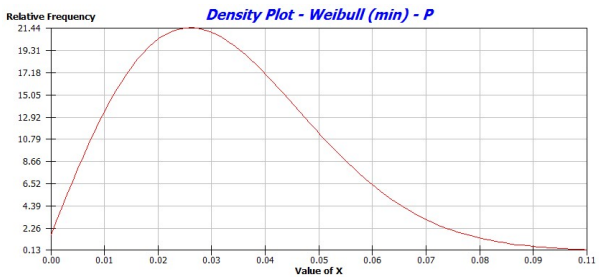

Fig.10. The optimal Weibull probability density function selected to describe the random variable p governing the natural possible volume of the imperfect ("weakened") adhesive material.

The probability density function of p presented in Fig. 10 fulfils the primary purpose of conducting a random analysis using the numerical "confidence intervals". Based on this function it is possible to randomly generate an experimentally determined level of internal structure imperfections in the material, distributed arbitrarily within the adhesive volume. This enables the calculation of FE models that incorporate imperfections at such levels and distributions, allowing for the numerical estimation of the expected rupture force of a batch of analyzed specimens. Subsequently, this approach can be used to assess the reliability of a joint assembled with the given adhesive, considering the randomly defined material imperfections.

4. APPLICATION OF THE RANDOM APPROACH TO AN ADHESIVE-BONDED SINGLE LAP JOINT RELIABILITY ASSESSMENT

4.1. The scope and aim of the analysis.

As mentioned in the preceding section, the presented analyses can be used to identify the random performance of real-life adhesive-bonded joints made with imperfect adhesive material. Both the authors' own analyses and the studies in the available literature highlight that variations in the adhesive layer have the greatest influence on the joint operation uncertainty. The natural variability of basic material parameters in the adhesive layer is significantly higher than the uncertainty level regarding the adherends [1, 2, 6, 13].

Therefore, the main aim of this study is to demonstrate the feasibility of using a probabilistic-based FE model that accounts for the random nature of the adhesive material in a simple adhesive-bonded joint. This approach allows for more realistic FE modeling of the joint and helps predict potential structural response variability. Furthermore, by applying an appropriate limit state, the impact of structural imperfections in the adhesive on joint reliability can be estimated.

Specifically, the paper focuses on analyzing a single-lap joint primarily subjected to uniaxial tension.

4.2. The geometry of the single lap joint specimen.

A single-lap joint, primarily subjected to uniaxial tension, is considered. The joint consists of two aluminum sheets bonded together with an adhesive overlay. The layout of the joint is shown in Fig. 11.

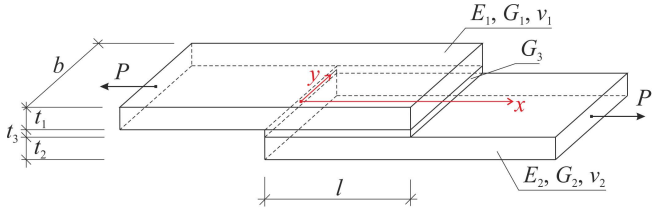

Fig.11. The layout of the geometry and material parameters of the investigated single-lap adhesive-bonded joint.

The joint has a width of b=25.4 mm and a length of l=25.4 mm. The overall length of the connection is chosen individually to ensure proper assembly of the specimen in the testing machine jaws and to accurately reflect the set boundary conditions.

Both adherend sheets are identical, each with a thickness of t_1=t_2=1.62 mm. They are made of AA-6063-T4 aluminum alloy, with the following material parameters: Young's modulus, E_1=E_2=68.3 GPa; Poisson's ratio, ν_1=ν_2=0.34; ultimate strength under axial tension, f_{1u}=f_{2u}=160 MPa. These parameters are adopted in accordance with EN485-2 and [12].
The adhesive used is the same as in the previous analysis: 3M Scotch DP490 synthetic epoxy adhesive, characterized by the material parameters listed in Subsection 3.2. The thickness of the adhesive layer is t_3=0.25 mm.

4.3. The numerical FE model of the adhesive-bonded single lap joint.

A three-dimensional (3D) FE model of the adhesive-bonded single lap joint was created using ABAQUS FEA software. The entire specimen was modeled with 966,000 C3D8R finite elements (three-dimensional, 8-node hexahedral elements with reduced integration and hourglass control). The finite elements representing the adherends had dimensions of 0.2×0.2×0.4 mm, while the elements representing the adhesive had dimensions of 0.05×0.05×0.1 mm. This configuration results in a total of 625,000 elements representing the entire adhesive layer. The mesh was refined to balance computational accuracy and time.
An overview of the analyzed model is shown in Fig. 12, including a close-up view of the FE mesh in the domain of the adhesive-bonded joint.
Fixed boundary conditions were applied to both ends of the model, except for translation in the direction of the specimen's length at the end where the load was applied as 10 mm displacement (Fig. 12a). The load was applied incrementally, with a maximum increment of 0.01 in order to minimize possible convergence issues.

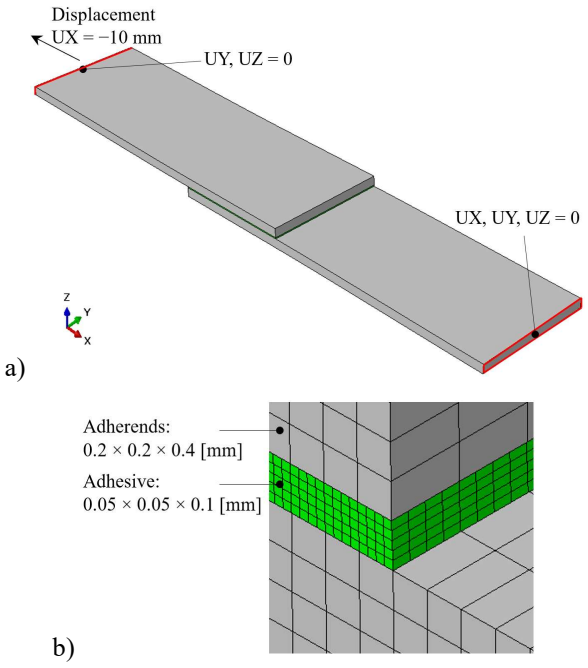

Fig.12. The 3D FE model of the adhesive-bonded single lap joint: (a) the full geometry with the boundary and loading conditions, and (b) a close-up view of the FE mesh of the adhesive.

The material parameters for the aluminum alloy elements, detailed in Subsection 4.2, are assumed constant, while those for the adhesive are modeled as either "nominal" or "weakened" (see Subsection 3.4). These parameters form an uncorrelated, conversed two-point scalar random field, as described in Section 2. The material parameters of the adhesive are input as centroid values, allowing the adhesive material volume to be described with the generated random fields (see Section 2 for details).The percentage of "weakened" elements in the entire target model domain is randomly generated from the previously derived Weibull probability density function given by Eq. (2).
In the final FEA study of the 3D numerical model, 26 samples were generated and computed.
For all samples, both the global and local mechanical response were investigated – the horizontal displacement of the entire joint (u=u_x) was assumed the primary global response and a relative horizontal displacement of the joint edge (u_h=u_{hx}) was adopted as the primary local response. The results of global and local joint response (for horizontal displacements) for selected numerical samples are given in Fig. 13.

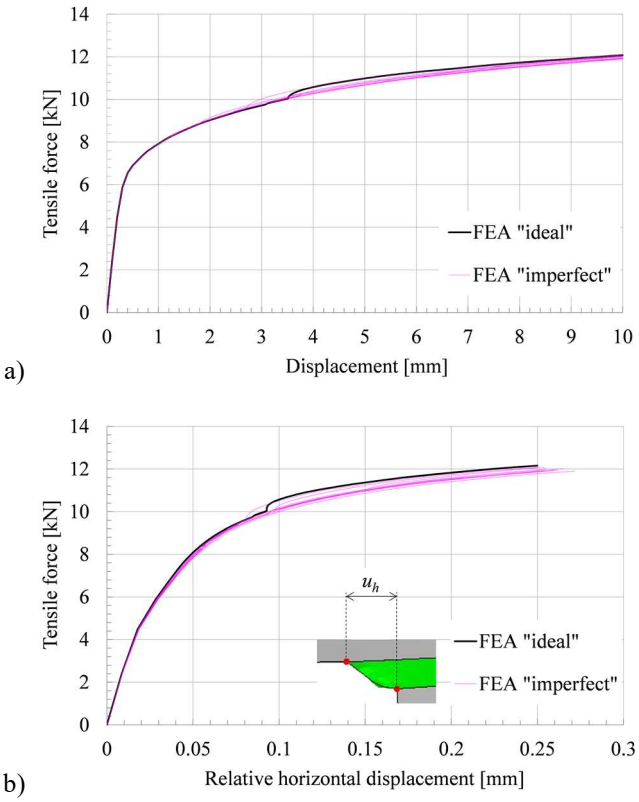

Fig.13. The mechanical response (horizontal displacements) of the adhesive-bonded single joint: (a) the global and (b) the local response. The responses of the ideal and imperfect 3D models are given for comparative purposes.

One FE model (sample) was assumed to be perfect, devoid of "weakened" elements in the entire FE domain of the adhesive, with an imperfection percentage p=0.00.
This "ideal" model determined the nominal tensile forces (F) in the "ideal" joint at specific levels of the global and local displacements, see Fig. 13a. Moreover, it constituted a reference point for subsequent randomly generated samples.

Selected numerical results for the "ideal" homogeneous variant of the single lap joint FE model are presented. The global structural response (displacements and stresses) is shown in Fig. 14. while a detailed view of the adhesive layer's local response (strains and stresses) is provided in Fig. 15.

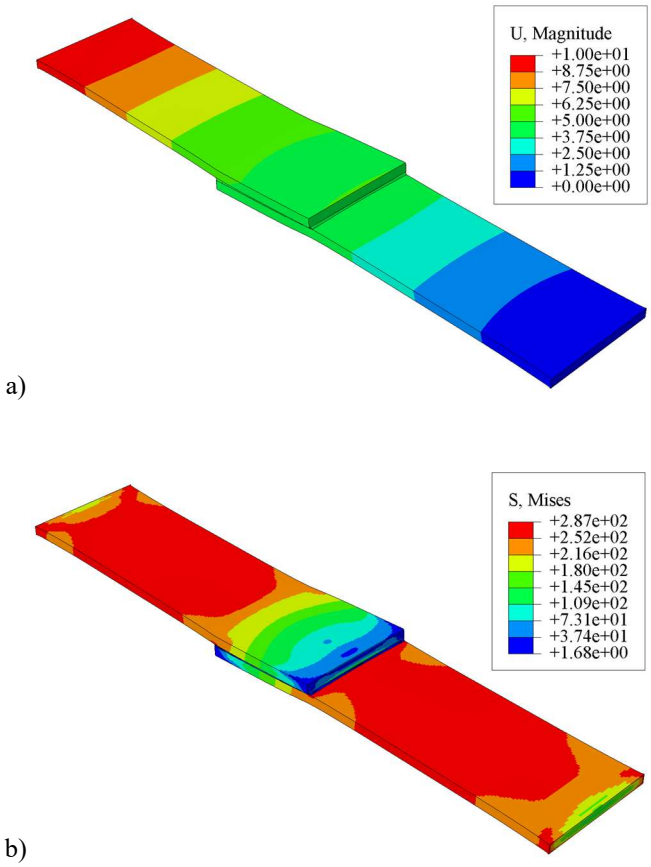

Fig.14. Numerical results for a homogeneous single-lap joint – global mechanical response: (a) displacement magnitude [mm] and (b) von Mises stress [MPa]

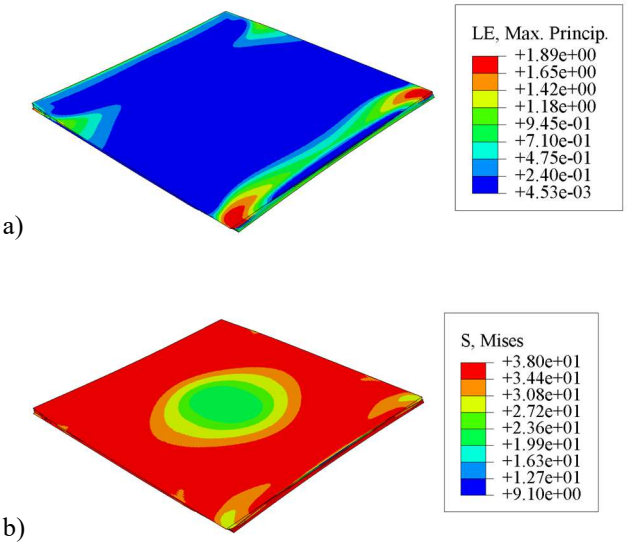

Fig.15. Numerical results for a homogeneous single-lap joint – local (adhesive layer) mechanical response: (a) maximum principal logarithmic strain [-] and (b) von Mises stress [MPa].

The next 25 samples were randomly generated based on the values of the level (percentage) of imperfections (p) derived from the properly identified Weibull PDF provided by Eq. (2). Please note, that p does not dictate a precise distribution of "weakened" elements throughout the volume, as it adheres to the nature of an uncorrelated random field. The same value of p may produce an entirely different layouts of structural imperfections. Nevertheless, 25 FE numerical random samples were all generated with unique p values. These values, the generated percentages of imperfections (unrelated to prior "confidence intervals") ranged from p_{min}=0.0006965 (a FE model with 436 "weakened" elements) to p_{max}=0.0812916 (a FE model with 50,808 "weakened" elements).

The local response of an exemplary random FE model, with a randomly generated imperfection level value of p=0.0511518 (including 31,969 "weakened" elements), is shown in Fig. 16.

For the random samples, not only the local mechanical response of the single lap joint was investigated, see Fig. 13b, the global response was also examined. However, only the local response, as shown in Figs. 16 b-c, served as the basis for the subsequent assessment of the probabilistic parameters of the joint's random structural response, useful in reliability calculations.

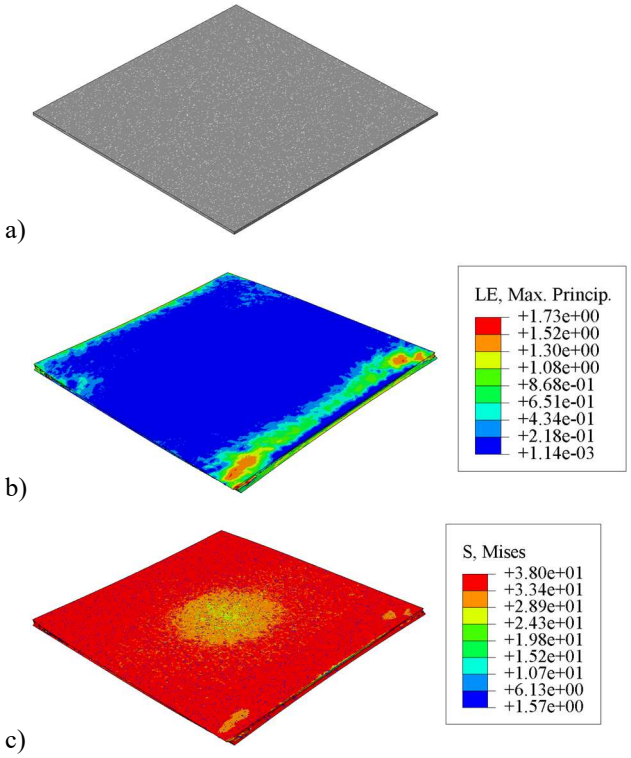

Fig.16. Numerical example of a non-homogeneous single-lap joint adhesive layer (a) distribution of the imperfections in the adhesive volume at imperfection level p=0.0511, (b) maximal principal logarithmic strain [-], and (c) von Mises stress [MPa].

It should be noted, that in assessing the local response, a criterion was introduced: the ultimate tensile force (F) induced in the joint is considered to cause a relative horizontal displacement of the joint edge equal to the thickness of the adhesive layer (u_h=u_{hx}=0.25 mm). It is believed that the mechanical behavior of the adhesive changes abruptly when its edges reach a 45° skewness, constituting a failure scenario.

4.4. Assessment of probabilistic parameters of the local structural response of 3D single lap joint FE model.

Based on the numerical calculations, the tensile forces in the adhesive-bonded single lap joint FE model can be summarized. The ultimate tensile force (F) for a "nominal" adhesive material F_{id}=12.16 kN, serves as the reference result for the local response of the joint.

The random numerical samples yield tensile forces for the local criterion ranging from $F_{num,min}$=11.681 kN to $F_{num,max}$=12.158 kN. The mean value of the 25 analyzed samples is μ_{Fnum}=11.977 kN (98.5% of F_{id}), with a small standard deviation of σ_{Fnum}=0.132 kN (coefficient of variation $v_{Fnum}=\sigma_{Fnum}/\mu_{Fnum}$ =0.011). This suggests that the impact of imperfections on the joint's performance is negligible. However, this insight is only valid for the specific type of adhesive, joint geometry, and the adopted probabilistic modeling of the adhesive layer considered in this study.

In Fig. 17, the results of numerical tests on joints with random material imperfections are shown as data points. Each data point represents a Weibull-based random imperfection level (p) and the corresponding computed tensile force (F).

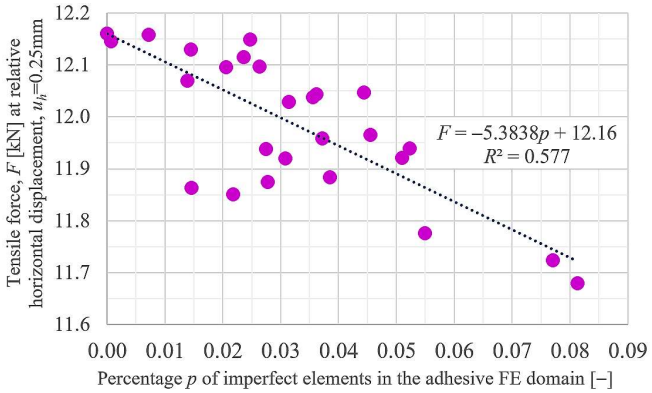

Fig.17. The results from the local response assessment of FE models, where the adhesive layer is assumed to be an uncorrelated random field, are presented along with a linear approximation of the response relationship.

The relationship between the imperfection level (p) and the axial tensile force (F) in the local approach, as plotted in Fig. 17 for specimens from numerical simulations of the random FE models, was additionally determined by assuming a linear approximation of the obtained data. The approximation yielded a determination coefficient R^2=0.577 and a correlation coefficient r=0.759, which are acceptable values considering the very limited data population and significant dispersion.

4.5. Determination of the limit state function for the adhesive-bonded joint.

Properly designed adhesive-bonded joints primarily experience tensile/compressive or shear stresses, ensuring the distribution of force across the entire bonding area. However, separating and peeling forces may concentrate the load at the edges, potentially leading to premature de-bonding.

To ensure the durability of the adhesive bond, it is important to consider the results of numerical tests that show significant deformation (skewing) of the adhesive layer (u_h=t_3= 0.25 mm). This deformation makes peeling (measured as force per unit length) highly probable. Therefore, the operational reliability of the adhesive bond should be evaluated to address this issue.

Based on calculations presented in Subsection 4.4, as the amount of imperfect material in the joint increases, the joint's strength decreases linearly. Therefore, a serviceability criterion for the joint can be established such that the axial force should not fall below a limit value, which would cause the relative strain of the entire joint to reach its limit ε_{lim}=0.01 (25% of total strain at rupture, ε_{3u}=0.04).

Using the formula for relative joint elongation, a specific value of the permissible value of the tensile force in the imperfect joint (N_{perm}) can be calculated, as shown in Eq (3):

$$N_{perm} \leq \varepsilon_{lim} EA_{joint} = 10.06 \text{ kN} \qquad (3)$$

If the level of imperfections is sufficiently high to reduce the force transmitted by the joint to the value specified in Eq. (3), in the scenario where the relative horizontal displacement of the joint edge equals the thickness of the adhesive layer (u_h=u_{hx}=0.25 mm), it indicates that the joint will undergo excessive deformation beyond the acceptable tolerance. This could lead to de-bonding or peeling, resulting in a loss of load-bearing capacity and ultimately causing the failure of the adhesive-bonded joint. Therefore, conducting an operational reliability assessment using the aforementioned value is essential and appropriate.

By considering the proposed permissible value of the tensile force in the imperfect joint, N_{perm}, given in Eq. (3), the established relationship between the mechanical response of the joint, and the linear approximation function of the input variable $F(p)$, the limit state function (LSF) can be expressed by Eq. (4):

$$\begin{aligned} LSF &= F(p) - N_{perm} \\ &= -5.3838p + 12.16\ [\text{kN}] - 10.06\ \text{kN} \\ &= 2.1 - 5.3838p[\text{kN}] \end{aligned} \qquad (4)$$

Using the constructed limit state function, given in Eq. (4), a reliability analysis of the potential failure of the adhesive-bonded joint can be conducted. The calculations were performed using the First Order Reliability Method (FORM) [14] within the COMREL 9.0 commercial software. This method was chosen for its ability to optimally estimate the reliability index with a linear limit state function. The Cornell technique [15] was subsequently used to assess the value of the reliability index for a linear random problem:

The assessed reliability index of the joint is $\beta(p)$=13.548. This is a very high value that indicates an extremely low probability of delamination for the considered bond. This conclusion is based on the specific type of adhesive used, the given joint geometry, and the probabilistic modeling of the adhesive layer.

5. CONCLUSIONS

The presented analysis demonstrates that the mechanical response of test adhesive-cast specimens or entire adhesive-bonded joints can be accurately simulated using FE software. This is achieved by incorporating the imperfect nature

of the internal structure of the adhesive through the random FE modelling incorporating uncorrelated random fields.

Key findings of the paper include:

- Modeling imperfections with random fields is appropriate, and the presented FE models incorporate varying degrees of adhesive material imperfections, represented as uncorrelated random fields converted to two-point scalar fields. This conversion enables the implementation of the proposed random approach. This method of modeling spatial random data on imperfections has been successfully used in previous analyses [11] and has also been applied to thin-walled structures, e.g. in [16, 17].
- Correlation between experimental and numerical results was established. In the FE analysis of adhesive material dogbone specimen, a successful match was observed between the structural responses from experimental tests and numerical simulations. This correlation, achieved through the determination of the so-called "confidence intervals" enabled the identification of the mechanical response of the adhesive and the estimation of the potential percentage of imperfect material in the real-life specimen.
- A justified and appropriately imperfect random material model was successfully introduced to represent the entire adhesive volume for FE modeling of adhesive-bonded joints. This model is based on the probability density function of the imperfection level random variable p, which governs the volume of imperfect material. The values of p were computed and calibrated based on tests conducted on real-life adhesive specimens. Consequently, a FE model that assumes an appropriate degree of adhesive layer weakening was created and analyzed, aligning with the real-life quality of joint preparation.
- A tailored imperfection assessment enabled a detailed investigation of the response variation of the entire joint and was found crucial for accurately predicting the operational reliability of the adhesive-bonded element, despite its non-idealized nature. Using simple probabilistic tools, future studies can also account for de-bonding or peeling failures, allowing for a genuine assessment of the probability of such failures.

Identifying and understanding the uncertain performance of adhesive material through random model analysis and quantifying the potential variation in the mechanical response of the adhesive-bonded joint are crucial. The proposed random field-based FE model helps mitigate the risks associated with adhesive joint failures.

This approach enhances the safety and reliability of real-life adhesive-bonded structures.

ACKNOWLEDGEMENTS

Financial support from the National Science Centre, Poland, under grant 2023/07/X/ST8/00497 titled "Failure analysis in a single-lap adhesive joint of thin sheets" within the "MINIATURA 7" program is gratefully acknowledged.

REFERENCES

[1] M. Kujawa, A. Cazzani, Ł. Smakosz, V. Konopińska-Zmysłowska, K. Winkelmann, F. Jan and C. Szymczak, "The Idea of Using Adhesive Bonds in Shaping of Cold-formed Thin-walled Beam-columns", in *Sixty Shades of Generalized Continua. Advanced Structured Materials 170*, 1st ed., H. Altenbach et al., Eds. Cham: Springer, 2023, pp. 449–462, doi: 10.1007/978-3-031-26186-2_28.

[2] S. Omairey, N. Jayasree and M. Kazilas, "Defects and uncertainties of adhesively bonded composite joints", *SN Applied Sciences*, vol. 3, pp. 769, 2021, doi: 10.1007/s42452-021-04753-8.

[3] F. Mortensen and O.T. Thomsen, "Analysis of adhesive bonded joints: A unified approach", *Composites Science and Technology*, vol. 62, no. 7–8, pp. 1011–1031, 2002, doi: 10.1016/S0266-3538(02)00030-1.

[4] A.P. Pisharody, B. Blandford, D.E. Smith and D.A. Jack, "An experimental investigation on the effect of adhesive distribution on strength of bonded joints", *Applied Adhesion Science*, vol. 7, pp. 6, 2019, doi: 10.1186/s40563-019-0122-y.

[5] X. Wei, Y. Huichen and T. Chunhu, "Influence of randomly distributed adhesive properties on the overall mechanical response of metallic adhesively bonded joints", *International Journal of Adhesion and Adhesives*, vol. 52, pp. 48–56, 2014, doi: 10.1016/j.ijadhadh.2014.04.001.

[6] R. Jairaja and G. Narayana Naik, "Weak bond effects in adhesively bonded joints between the dissimilar adherends", *The Journal of Adhesion*, vol. 97, no. 3, pp. 760–782, 2019, doi: 10.1080/00218464.2019.1702027.

[7] J. Kuczmaszewski. *Fundamentals of metal-metal adhesive joint design.* Lublin: Lublin University of Technology, Polish Academy of Sciences, Lublin Branch, 2006.

[8] E. Wojtczak, M. Rucka and M. Knak, "Detection and imaging of debonding in adhesive joints of concrete beams strengthened with steel plates using guided waves and weighted root mean square," *Materials*, vol. 13, no. 9, pp. 2167, 2020,doi: 10.3390/ma13092167. vol. 68.

[9] M. Nitka and J. Tejchman-Konarzewski, "A three-dimensional meso-scale approach to concrete fracture based on combined DEM with x-ray micro-CT images," *Cement and Concrete Research*, vol. 107, pp. 11–29, 2018, doi:10.1016/j.cemconres.2018.02.006.

[10] W. Moćko, J. Janiszewski, J. Radziejewska and M. Grązka, "Analysis of deformation history and damage initiation for 6082-T6 aluminium alloy loaded at classic and symmetric Taylor impact test conditions," *International Journal of Impact Engineering*, vol. 75, pp. 203–213, 2015, doi: 10.1016/j.ijimpeng.2014.08.015.

[11] K. Żyliński, K. Winkelmann and J. Górski, "The Effect of the Selection of Three-Dimensional Random Numerical Soil Models on Strip Foundation Settlements," *Applied Sciences-Basel.*, vol. 11, pp. 7293, 2021, doi: 10.3390/app11167293.

[12] M. Piekarczyk and R. Grec, "Application of adhesive bonding in steel and aluminum structures", *Archives of Civil Engineering*, vol. 58, no. 3, pp. 309–329, 2012, doi: 10.2478/v.10169-012-0018-8.

[13] E.W. Kuenzi and G.H. Stevens. *Determination of mechanical properties of adhesives for use in the design of bonded joints.* Washington D.C.: The United States Department of Agriculture, Forest Service, Forest Products Laboratory, Volume 11, 1963.

[14] A.M. Hasofer, N.C. Lind. "An Exact and Invariant First-Order Reliability Format", *ASCE Journal of Engineering Mechanics Division* 1974, Vol. 100, pp. 111–121, doi: 10.1061/JMCEA3.0001848

[15] C.A. Cornell. *A probability-based structural code.* Detroit: American Concrete Institute Journal, Volume 11, Issue 12, 1969, pp.974-985, doi: 10.14359/7446.

[16] M. Gołota, J. Górski, T. Mikulski and K. Winkelmann, "Influence of geometric imperfections on capacities of silo structures loaded with pressure below atmospheric" in *Shell Structures: Theory and Applications Volume 2 - Proceedings of the 9th International Conference on Shell Structures: Theory and Applications, SSTA 2009*, 1st ed., W. Pietraszkiewicz and I. Kreja, Eds. London: CRC Press/Balkema, 2010, pp. 287–290, doi: 10.1201/9780203859766.CH64.

[17] K. Żyliński and J. Górski, "Probabilistic estimation of diverse soil condition impact on vertical axis tank deformation*", Bulletin of the Polish Academy of Sciences - Technical Sciences*, vol. 71, pp. 144576, 2023, doi: 10.24425/bpasts.2023.144576.